LA-SUB--96-101

Correlation of Zeno (Z = 1) Line for Supercritical Fluids with Vapor-Liquid Rectilinear Diameters

Dor Ben-Amotz and Dudley R. Herschbach
Corporate Research Science Laboratories, Exxon Research and Engineering Company, Annandale, NJ 08801

Abstract

For a wide range of subtances, extending well beyond the regime of corresponding states behavior, the contour in the temperature-density plane along which the compressibility factor $Z = P/\rho kT$ is the same as for an ideal gas is nearly linear. This $Z = 1$ contour, termed the Zeno line, begins deep in the liquid region and ascends as the density decreases to the Boyle point of the supercritical fluid, specified by the temperature T_B for which $(dZ/d\rho)_T = 0$ as $\rho \rightarrow 0$; equivalently, at T_B the second virial coeffcient vanishes. The slope of the $Z = 1$ line is $-B_3/(dB_2/dT)$, in terms of the third virial coefficient and the derivative of the second, evaluated at T_B. Previous work has examined the Zeno line as a means to extend corresponding states and to enhance other practical approximations. Here we call attention to another striking aspect, a strong correlation with the line of rectilinear diameters defined by the average of the subcritical vapor and liquid densities. This correlation is obeyed well by empirical data for many substances and computer simulations for a Lennard-Jones potential; the ratios of the intercepts and slopes for the Zeno and rectilinear diameter lines are remarkably close to those predicted by the van der Waals equation, 8/9 and 16/9, respectively. Properties of the slightly imperfect fluid far above the critical point thus implicitly determine the diameter of the vapor-liquid coexistence curve below the critical point.

DISCLAIMER

I. Introduction

For a high-density liquid in equilibrium with its low-density vapor, the shape of the coexistence curve in the temperature-density plane exhibits two features with intriguing generality, recognized empirically for more than a century.[1] According to the "law of rectilinear diameters," the *average density* $\bar{\rho} = (\rho_L + \rho_V)/2$ varies almost linearly over a substantial temperature range below the critical point. In contrast, the *density difference* $\Delta\rho = \rho_L - \rho_V$ is governed by a characteristic fractional exponent. Both $\bar{\rho}$ and $\Delta\rho$ become singular as the critical temperature is approached.[1,2] The modern theory of phase transitions has shown these features to be much more general than corresponding states behavior. Provided the forces are repulsive at close distances, become attractive further out, and vanish sufficiently rapidly at long range, both the critical exponent and the approximate rectilinearity of the average density are independent of any quantitative aspects of the intermolecular forces.

Much less well known is another striking feature located well outside the liquid-vapor coexistence region, a nearly linear empirical relation stretching over a wide domain of the temperature-density plane. This is the contour with $Z = 1$, termed here the Zeno line, along which the compressibility factor $Z = P/\rho kT$ is the same as for an ideal gas. The $Z = 1$ line extends from the dense liquid region to the Boyle point of the dilute fluid, where the density $\rho \to 0$ and the temperature T_B is such that the second virial coefficient B_2 vanishes. The slope of the $Z = 1$ line is determined by the ratio of the third virial coefficient B_3 to dB_2/dT at T_B.

This line has a long and curious history.[3] It seems first to have been recognized in 1893 by Amagat,[4] but independently rediscovered in 1906 by

Batschinski,[5] in 1963 by Morsy,[6] in 1967 by Holleran,[7] in 1983 by Powles,[8] and probably by others (as well as the present authors). Applications include extended treatments of corresponding states,[9,10] analysis of interrelations among virial coefficients,[11,12] and improved approximations for equations of state.[13,14] The nomenclature has remained unsettled, however. Terms previously used include "unit compressibility law" or line[7] (awkward, especially since the compressibility factor is meant, not the compressibility); "zero order characteristic" curve[14] (uniformative); and "Boyle line" or curve[8] (invites confusion with the accepted name for a quite different locus[15] defined by $(\partial Z/\partial P)_T = 0$). We suggest the name "Zeno line" (derived from Z = one). This emphasizes the paradoxical character of the arrowlike linearity, which implies that properties of the low density fluid somehow dictate the balance of repulsive and attractive forces even at quite high densities.

Our chief aim in this paper is to call attention to another paradoxical aspect of the Zeno line. We find a strong correlation with the line of rectilinear diameters, accurately obeyed by empirical data for many substances and computer simulations for a Lennard-Jones potential. The ratios of the intercepts and slopes of the Zeno and rectilinear diameter lines are close to values predicted by the van der Waals equation, 8/9 and 16/9, respectively. This correlation indicates a remarkable kinship among the Boyle point, which pertains to supercritical dilute gas, and both the subcritical two-phase region and the liquid domain.

In Sec. II we note some heuristic aspects and illustrate the Zeno contour with data for several representative substances; this considerably augments previous examples[7,8] and offers a modest complement to the extensive documentation available for the rectilinear diameter line.[16] In Sec. III we exhibit the Zeno-diameter correlation, as exemplified by empirical data, computer simulation results for the Lennard-Jones potential, and the van der Waals equation. In Sec. IV we illustrate some applications of this correlation.

II. Hard and Soft Fluid Regimes

Many aspects of the modern theory of fluids affirm the venerable view of van der Waals, which contrasted the roles of repulsive and attractive forces.[17,18] In the gas phase at low ρ and modest T, initial deviations from the ideal gas limit result chiefly from attractive forces, whereas as ρ and T increase repulsion becomes dominant. In the liquid phase at high ρ and low T, repulsive hard-spheres offer a good zeroth order model for the major excluded volume and packing effects; the attractive forces provide a uniform cohesive background but have little influence on the liquid structure or dynamics. However, the attractive forces become much more prominent when the vapor-liquid coexistence region and particularly the critical point are approached.

In particular, the competition between repulsive and attractive forces is exemplified in vibrational frequency shifts of molecules induced by solvation or pressure. Studies[19] of such shifts as a means to determine effective hard sphere diameters and attractive force constants led us to examine approximation schemes suitable for *hard fluid* and *soft fluid* regimes, corresponding to dominance of repulsive or attractive forces, respectively. This suggested considering the compressibility factor as a criterion, since $Z > 1$ when repulsion is dominant and $Z < 1$ when attraction is dominant.

Figure 1 shows the typical pattern of isotherms for Z as a function of density.[20] For temperatures below the Boyle temperature T_B, the isotherms initially swoop below $Z = 1$ but eventually climb steeply above as the density increases. At the Boyle temperature, the slope $(\partial Z/\partial \rho)_T$ vanishes for $\rho \rightarrow 0$ and at higher temperatures the isotherms lie entirely above the $Z = 1$ asymptote. For the locus of points (T, ρ) where $Z = 1$ the attractive and repulsive contributions balance and the fluid imitates an ideal gas.

This $Z = 1$ locus, the Zeno contour, is analogous to the "glory" trajectory

familiar in elastic scattering of molecules, for which long-range attraction and short-range repulsion balance and produce no net deflection of the relative velocity vector.[21] Replotting Z-isotherms versus $\rho^{-1/3}$ allows a heuristic comparison with the intermolecular potential. Figure 2 illustrates this. At high density (small r), both Z and the intermolecular potential V(r) increase steeply, exhibiting harsh repulsion. At low density (large r), both Z and V(r) flatten out, displaying the long-range attraction and approaching isolated molecule asymptotes. At intermediate densities (and moderate temperatures) Z like V(r) has a minimum. The density at which Z = 1 is seen to correspond to a radius r_{Zeno} appreciably larger than the core radius σ for which $V(\sigma) = 0$ and as T increases r_{Zeno} moves outwards; likewise, the mimimum in Z lies well outside that in the potential.

A. Empirical Results

Figure 3 shows the reduced density-temperature phase diagram of methane. In addition to the familar regimes of vapor, liquid, solid and phase coexistence, we indicate the hard and soft fluid regimes. Several constant Z-contours are drawn through experimental points. The striking linearity of the Z = 1 contour is evident as well as the drastic "peeling away" of the neighboring Z-contours. This diagram is qualitatively typical for many substances and quantitatively a good approximation for some exhibiting corresponding states behavior. Three kinds of fixed points have special roles: (i) the triple point(s), at which vapor, liquid, and solid coexist with distinct densities but a common pressure and temperature; (ii) the critical point, above which there is no vapor-liquid phase transition; and (iii) the Boyle point, at which the second virial coefficient of the fluid vanishes. To a fair approximation,[2,16] the rectilinear diameter line connects the critical point to the mean of the vapor and liquid triple points; likewise, the Zeno line stems from the Boyle point down to the vicinity of the mean of the liquid and solid triple points. The linearity indicates that the balance between repulsive and

attractive contibutions is somehow maintained in a uniform fashion between the dilute fluid regime and the dense, condensed phase regime.

Many other examples of linear or nearly linear Zeno lines have been found. Figure 4 shows some representative data.[20] The most extensive data are available for argon and show that the Z = 1 contour is remarkably linear all the way from the triple point temperature to the Boyle point. The linearity is also very good for N_2, CH_4, and n-alkanes, whereas slight negative curvature appears for H_2O. Table I lists the slope and intercept for least-square fits of Zeno lines to the data; correlation coefficients are typically 0.9990, but 0.99997 for Ar and 0.997 for H_20. Since in Figs. 3 and 4 we have scaled temperature and density to the critical point, the Zeno line (and other Z-contours) should be the same for substances obeying corresponding states, such as Ar, N_2, and CH_4. The Zeno lines indeed overlap quite closely for Ar and CH_4, less so for Ar and N_2, and differ considerably for the other pairs of substances. The near linearity of the Zeno line thus appears to be a typical property for a wide range of substances, extending well beyond the regime of corresponding states behavior.

B. Relation to virial coefficients

In the low-density region, the general pattern of the Z-contours seen in Fig. 3 and the special status of Z = 1 may be derived from the virial expansion,

$$Z = 1 + B_2\rho + B_3\rho^2 + \ldots \qquad (1)$$

where the virial coefficients B_k are functions of temperature. The thermodynamic relation

$$(\partial T/\partial \rho)_Z = - (\partial Z/\partial \rho)_T/(\partial Z/\partial T)_\rho$$

yields

$$(\partial T/\partial \rho)_Z = - [B_2 + 2B_3\rho + \ldots]/[B'_2\rho + B'_3\rho^2 + \ldots] \qquad (2)$$

where the primes denote temperature derivatives, $B'_k = dB_k/dT$. On eliminating B_2 by use of Eq.(1), we find the slope as $\rho \rightarrow 0$ is given by

$$(\partial T/\partial \rho)_Z = - [(Z - 1)/\rho^2 + B_3 + 2B_4\rho + \ldots]/B'_2 \qquad (3)$$

Thus, for all contours of constant Z on a T-ρ diagram, the slope will become singular as $\rho \rightarrow 0$, *except* for the Z = 1 contour, for which the slope is $-B_3/B_2'$, evaluated at T_B. The temperature derivative B'_2 is positive (except for temperatures far above T_B, not considered here). Hence on approaching the ρ = 0 axis, a contour with Z > 1 will exhibit a steeply negative slope, with positive curvature, whereas a contour with Z < 1 will exhibit a steeply positive slope and negative curvature. This accounts for the "peeling away" pattern seen in Fig. 3 and the lonely approach of the Zeno line to the ρ = 0 axis.

Table II lists intercepts and slopes evaluated from T_B and virial coefficients. Because very few B_3 values are available, for this tabulation we used Lennard-Jones results, with potential parameters determined from B_2 data.[23] The T_B(LJ) values may be compared with the results listed in Table I, obtained from experimental B_2 coefficients or from the intercepts of the Zeno lines; this serves to indicate which substances deviate substantially from the LJ potential. Figure 5 compares the intercepts and slopes obtained from virial coefficients with the results of Table I. The agreement is surprisingly good, considering that the virial analysis pertains solely to properties of the low-density gas. The empirical Zeno intercept is typically within ± 2% of the T_B obtained from the experimental B_2. The empirical slope correlates much less well with the LJ virial results; typically the agreement is within about ±10 %, but far worse in some cases (e.g., for CO_2 and C_2H_6) due to the inadequacy of the LJ potential.

III. Kinship of Zeno and Rectilinear Diameter Lines

As illustrated in Fig. 3, extrapolating the rectilinear diameter (RD) line into the supercritical fluid region typically gives an intercept on the ρ = 0 axis somewhat below that for the Zeno line whereas the slope of the RD line is always much steeper. Table I includes these parameters and Fig. 6 shows that good linear correlations hold for both the intercept and slope. The data for the 13

systems included represents all cases for which we have thus far obtained both vapor-liquid equilibrium data and empirical Zeno lines. Least-squares fits give 0.866 and 1.802, respectively, for the ratio of intercepts and the ratio of slopes, RD to Zeno. The correlation coefficients are 0.990 and 0.996, respectively.

Note that in Table I and Fig. 6 the Zeno and RD lines were evaluated using absolute temperatures and densities, before normalizing to the critical parameters. This was done to avoid introducing uncertainties due to errors in the T_c and ρ_c values. Accordingly, the RD lines obtained are not constrained to pass through the critical point. That constraint requires the sum of the slope and intercept, in reduced units, to equal unity. For the unconstrained data, the mean slope + intercept is 1.01, with ± 0.06 as the standard deviation. This is pertinent also in comparing our RD lines with an approximation derived by Guggenheim[22] from a corresponding states analysis, $(\tilde{\rho} - 1) = 0.75[1 - (T/T_c)]$. From Table I we find that the coefficient, given by the negative reciprocal of our slope, has an mean value of 0.83 with ±0.14 as the standard deviation. Values ranging from 0.68 to 1.09, with a mean of 0.94 are found for 27 substances compiled by Partington.[16]

Table I also includes parameters determined from extensive Monte Carlo computer simulations for a Lennard-Jones potential.[24,25] The Z = 1 contour is quite linear over a wide T-ρ range; the correlation coefficient is 0.9995 for the least-squares fit. (Incidentally, we find that the much more limited simulation data[26] for a two-dimensional L-J potential yields, within its scatter, the same Zeno line.) The phase diagram obtained is very similar to Fig. 3 and the corresponding ratios for the intercepts and slopes are 0.875 and 1.823, respectively, RD to Zeno.

The van der Waals equation yields explicit formulas (derived in the Appendix) for the (rigorously linear) Zeno line:

$$T/T_c = 27/8 - (9/8)\rho/\rho_c, \qquad (4)$$

and (a nominally linear approximation) for the rectilinear diameter line:

$$T/T_c = 3 - 2\bar{\rho}/\rho_c. \qquad (5)$$

The ratio of intercepts and slopes thus is 8/9 = 0.889 and 16/9 = 1.778, respectively. These values are close to the empirical and Lennard-Jones results, although the van der Waals equation is quantitatively extremely poor except for a very dilute gas. The correspondence is especially striking in the density intercepts (at T = 0), given by -I/S in the notation of Table I. For the 13 systems, the ratio of these density intercepts is 2.01 ± 0.10, Zeno to RD, whereas the van der Waals result is exactly two. This congruence in the ratios suggests that the Zeno and rectilinear diameter lines can for many purposes be regarded as equivalent.

Figure 7 compares the Zeno and rectilinear diameter lines for the Lennard-Jones potential and the van der Waals equation. Also shown are computer simulation results for a hard core + square well potential;[18,27] these data are more sparse and noisy, but indicate the Z = 1 contour has appreciable curvature. The Zeno lines for the LJ and SW potentials (shown solid) are not fitted to the points but rather computed from virial coefficients,[23] to provide another comparison. Curiously, at large densities the square well results appear to approach the van der Waals lines, both for the Z = 1 contour and the rectilinear diameters. The square well potential is doubtless qualitatively unrealistic, but serves to show that the position of the Zeno contour, its linearity, and its correlation with rectilinear diameters all indeed reflect the shape of the intermolecular interaction potential.

IV. Discussion

As reliable empirical regularities spanning a wide range of temperature, density, and molecular structure, both the Zeno and RD lines deserve attention as means to extend corresponding states and to enhance other practical approximations. Very little experimental data is required to fix these lines and it

can come from properties of either the dilute gas or the dense fluid or liquid. In particular, the correlation of Fig. 6 enables use of the extensive vapor-liquid equilibrium data[16,20] to predict properties of the supercritical fluid. For instance, the Boyle points of larger or more strongly interacting molecules are often unavailable, since these tend to fall above 1000 °K, where the molecules decompose. Here we illustrate two other applications of this correlation, to obtain estimates for the critical density or the triple point liquid density. There are many other options, exemplified in previous discussions of the Zeno line.[7-15]

A. From Zeno or RD to Critical Density

The critical density is much more difficult to measure than the critical temperature. Often tabulated values of ρ_c show large scatter or are missing altogether. For instance, for methane the tabulated ρ_c varies as much as 15% from the value accepted as best,[20] whereas for T_c the standard deviation is only 0.1%. In such cases, it is useful to estimate ρ_c from T_c and the rectilinear diameter line. The correlation with the Zeno line allows this even in the absence of data for the vapor-liquid equilibrium. For example, from the Zeno line for methane in Table I and the correlation of Fig. 6 we obtain

$$I_{RD} = 0.866 I_Z = 438\ ^{o}K \text{ and } S_{RD} = 1.802 S_Z = -42.3\ K\ nm^3$$

for the intercept and slope of the rectilinear diameter line. Then with $T_c = 190.5$ °K we find $\rho_c \approx 5.83\ nm^{-3}$. This estimate is within 4% of the accepted value, $\rho_c = 6.05\ nm^{-3}$, despite the modest accuracy of our estimates of I_{RD} and S_{RD}, which differ by 3% and 9%, respectively, from the values of Table I obtained directly from vapor-liquid data.

B. From RD or Zeno to Triple Point Liquid Density

As seen in Fig. 3, the Z = 1 line passes near the liquid triple point. It cannot pass through that point, as shown by the following argument. The vapor phase in equilibrium with the liquid at P_t and T_t is a low density, nearly ideal gas, so $Z_t(vap) \approx 1$. For the liquid phase, however, ρ_t is of the order of 1000-fold

greater; thus, since P_t and T_t are fixed, $Z_t(\text{liq}) \approx 10^{-3}$. Table III lists triple point data. We find that the density of the liquid on the Zeno line at T_t is about 5-10% above the triple point liquid density. Since the density of the solid at T_t is about 15% higher than the liquid, this makes the density for Z = 1 roughly comparable to the mean of the liquid and solid triple points, although the Zeno line exhibits a discontinuous density jump at the liquid-solid transition.[10]

Inspection of the phase diagram suggests a simple means to estimate $\rho_t(\text{liq})$ from the RD and/or Zeno lines. Since $\rho_t(\text{vap})$ is negligibly small compared with $\rho_t(\text{liq})$, the latter density lies on a line with intercept I_{RD} and slope $S_{RD}/2$. We refer to this as the "TPL line." The liquid density at the triple point thus may be estimated from

$$\rho_t(\text{liq}) = 2(T_t - I_{RD})/S_{RD} \qquad (6)$$

As seen in Table III, estimates from this formula are in 3 of the 4 examples within ±1.5% of experimental values for the triple point liquid density.

Finally, we note another striking aspect linking the Zeno and RD lines to the TPL line. For the examples at hand, the density intercept (at T = 0) for the TPL line appears to coincide with that for the Zeno line. Since these intercepts are given by $-2I_{RD}/S_{RD}$ and $-I_Z/S_Z$, respectively, this result is equivalent to the observation that the density intercept of the Zeno line is twice that for the RD line. As noted in the discussion of Fig. 6, for all the systems in Table I this holds within ±5% (and exactly for the van der Waals equation). Accordingly, the liquid triple point lies on a line (TLP) connecting the density intecept of the Zeno line with the temperature intercept of the rectilinear diameter line. On each of these three linked lines, which mark out a stylishly distorted letter "Z" on the T-ρ diagram, there resides one of the major characteristic points: the liquid triple point, the Boyle point, and the critical point, respectively.

It is tantalizing that these straight lines, stretching over much of the phase diagram, are governed to a surprisingly good approximation just by properties of

the slightly imperfect gas, T_B and the virial coefficient ratio $B_3(T_B)/B'_2(T_B)$. There appears to be a curious conspiracy among the higher virial terms to maintain these linear kinships, in accord with the proverb: "as the twig is bent, so grows the tree."

Acknowledgements

We are pleased to join in honoring Joshua Jortner and Raphy Levine, who so often have taken bold aim at central problems of chemical physics and adroitly launched rectilinear arrows or transforming thunderbolts, with exemplary lucidity, insight, and zest. We have enjoyed opportunities to discuss aspects of this work with Bernie Alder, Harry Drickamer, Stan Huang, Sabre Kais, Lawrence Pratt, Mac Radosz, and Ben Widom; we are especially indebted to David Johnston for his skill and persistence in searching the literature.

Appendix: Zeno and RD Lines from vdW Equation

The rigorous linearity of the Z = 1 contour in the T-ρ plane for the van der Waals equation was shown in 1906 by Batschinski[5] and later by others[7,8] but for convenient reference we include this as a preliminary to evaluating the rectilinear diameter line. The van der Waals equation in its customary form is

$$Z = PV/nRT = (1 - b\rho)^{-1} - (a/RT)\rho \qquad (A1)$$

where b is the excluded volume parameter and a the attractive energy density parameter. This may be recast as

$$Z = 1 + [b - (a/RT)]\rho + b^2\rho^2/(1 - b\rho) \qquad (A2)$$

The second term is now the second virial coefficient, which vanishes at the Boyle temperature, so $T_B = a/bR$. Along the Z = 1 contour,

$$[1 - (T_B/T)] + b\rho/(1 - b\rho) = 0 \qquad (A3)$$

and this gives the linear relationship,

$$T = (1 - b\rho)T_B. \qquad (A4)$$

At the critical point, $T_c = (8/27)T_B$ and $\rho_c = 1/3b$; thus we obtain Eq.(4) of the text.

Likewise, from the criterion $(\partial Z/\partial \rho)_T = 0$, we find the locus of minima for the Z-isotherms (as in Fig. 1) is parabolic

$$T = (1 - b\rho)^2 T_B \qquad (A5)$$

and the corresponding minimum on the isotherm is

$$Z = (T_B/T)^{1/2}[2 - (T_B/T)^{1/2}] \qquad (A6)$$

but these relations hold only for $T \geq T_c$.

The rectilinear diameter line is *not* rigorously linear for the van der Waals equation. Table IV gives the vapor and liquid densities for the coexistence curve,[8] the corresponding values of Z on the curve, and the mean density $\bar{\rho} = (\rho_L + \rho_V)/2$. The nominal approximation for the rectilinear diameter line is defined by the density intercept ($T = 0$, $\bar{\rho}/\rho_c = 3/2$) and the critical point; this gives Eq.(5) of the text. As seen in Table IV, the actual locus of ρ versus T deviates from linearity by up to about 1.4% (at T/Tc = 0.7); thus this locus is slightly bowed toward the vapor branch of the coexistence curve.

References

Present address: Department of Chemistry, Purdue University, West Lafayette, Indiana

Exxon Faculty Fellow from Harvard University, Department of Chemistry, 12 Oxford Street, Cambridge, Massachusetts 02138

1. B. Widom in *Fundamental Problems in Statistical Mechanics, Vol III*, ed. E.D.G. Cohen (North-Holland, 1975), pp.1-45.
2. R. E. Goldstein and A. Parola, *Acc. Chem. Res.* **22**, 77 (1989), and work cited therein.
3. H. Brandl, *Z. phys. Chem. (Leipzig)* **260**, 174 (1979).

4. E.H. Amagat, *Ann. Chim. Phys.* **6**, 29 (1893).

5. A. Batschinski, *Ann. d. Phys.* **19**, 307 (1906).

6. T.E. Morsy, Dissertation, TH Karlsruhe (1963).

7. E.M. Holleran, *J. Chem. Phys.* **47**, 5318 (1967).

8. J.G. Powles, *J. Phys.* **C16**, 503 (1983).

9. E.M. Holleran and G. Gerardi, *J. Phys. Chem.* **72**, 3559 (1968); **73**, 167, 528, 3700 (1969); *Cryogenics* **10**, 423 (1970).

10. V.B. Magalinskii and N.A. Glushkov, *Z. Fiz. Khim.* **53**, 914 (1979) [*Russ. J. Phys. Chem.* **53**, 515 (1979); *Izv. Vyssh. Uchebn. Zavedl, Fiz.*, **22**, 110 (1979).

11. E.H. Holleran and J.V. Sinka, *J. Chem. Phys.* **49**, 39 (1968); **55**, 4260 (1971).

12. W. Rudzinski, *J. Phys.* **A5**, 1642 (1972); W. Rudzinski and S. Sokolowski, *Surf. Sci.* **65**, 593 (1971); W.Rudzinski and J. Oscki, *Z. phys. Chem. (Leipzig)* **262**, 235 (1981).

13. E.H. Holleran and R. S. Jacobs, *Ind. Eng. Chem.* **11**, 272 (1972); *Cryogenics* **15**, 137 (1975).

14. J. Stephenson and H.K. Leung, *Phys. Chem. Liq.* **8**, 249 (1979).

15. J.S. Rowlinson, *Repts. Prog. Phys.* **28**, 169 (1965).

16. J.R. Partington, *Treatise on Physical Chemistry,* Vol. I (Longman, Green, 1949), p. 639.

17. J.P. Hansen and I.R. McDonald, *Theory of Simple Liquids*, 2nd Ed. (Academic Press, 1986).

18. B.J.Alder and C.E. Hecht, *J. Chem. Phys.* **50**, 2032 (1969); J.A. Barker and D. Henderson, *Rev. Mod. Phys.* **48**, 4045 (1980); D. Chandler, J.D. Weeks, and H.C. Andersen, *Science* **220**, 787 (1983), and work cited therein.

19. D. Ben-Amotz, M.R. Zakin , H.E. King, and D.R. Herschbach, J. Phys. Chem. **92**, 1392 (1988); M.R. Zakin and D.R. Herschbach, J. Chem. Phys. **89**, 2380 (1988), and work cited therein.

20. Sources for experimental data: (a) *Landolt Bornstein, Zahlenwerte und Funktionen*, Vol. 2, Part 1 and Part 2; Vol. 4, Part 4 (Springer, Berlin, 1971); (b) *International Critical Tables*, Vol. III (McGraw-Hill, 1928); (c)*International Thermodynamic Tables of the Fluid State*,Vol. 1-8 (Pergamon, 1979); additional data for CH_4 from: A. van Itterbeek, O. Verbeke, and K. Staes, *Physica* **29**, 742 (1963); for Ar from: J.M.H. Levelt, *Physica* **26**, 361 (1960); W.B. Streett and M.S. Constantino, *Physica* **75**, 283 (1974); for Ne from: H. Lippold, *Cryogenics* **7**, 243 (1967); W.B. Streett, *Cryogenics* **8**, 88 (1968); for Kr from: W.B. Streett and L.A.K. Staveley, *J. Chem. Phys.* **55**, 2495 (1971); M. Gehrig and H. Lentz, *J. Chem. Thermo.* **11**, 291 (1979).

21. R.D. Levine and R.B. Bernstein, *Molecular Reaction Dynamics and Chemical Reactivity* (Oxford, New York, 1987), pp. 69-71.

22. E.A. Guggenheim, *Thermodynamics* (North-Holland, Amsterdam, 1967), pp. 135-144.

23. J.O. Hirschfelder, C.F. Curtiss, and R.B. Bird, *Molecular Theory of Gases and Liquids* (J. Wiley and Sons, New York, 1954), pp. 158, 1114, 1116.

24. J.J. Nicolas, K.E. Gubbins, W.B. Streett, and D.J. Tildesley, *Mol. Phys.* **37**, 1429 (1979).

25. A.Z. Panagiotopoulos, *Mol. Phys.* **61**, 813 (1987).

26. J.A. Barker, D. Henderson, and F.F. Abraham, *Physica* **106A**, 226 (1981).

27. D.D. Carley, *J. Chem. Phys.* **78**, 5776 (1983).

Figure Captions

Fig. 1. Density dependence of isotherms for the compressibility factor Z of methane at various reduced temperatures, derived from experimental data.[20] Dashed curve pertains to Boyle temperature.

Fig. 2. Comparison of Lennard-Jones (6,12) potential for methane (ordinate at left, in ^{o}K) with compressibility factor (ordinate at right) isotherms.

Fig. 3. Phase diagram for methane, with experimental points for several Z-contours. Also shown is the line of rectilinear diameters in the vapor-liquid coexistence region, and its extrapolations (short-dashed lines).

Fig. 4. Zeno lines for Ar, N_2, CO_2, H_20 (at right) and normal alkanes (at left). Points are experimental data.[20] Ordinates for successive lines are displaced upwards by 0.5 units to avoid crowding. Solid lines are least-square fits, with intercept and slope given in Table I; dashed lines show Ar result for comparison.

Fig. 5. Correlation of parameters for Zeno lines. Empirical intercept (right ordinate scale, from least-square fits to Fig. 4 given in Table I) compared with Boyle temperature (lower abcissa, from second virial coefficient, T_B given in Table I); for line shown ordinate is 1.03 times abcissa and correlation coefficent is 0.9997. Empirical slope (left ordinate scale, from Table I) compared with Lennard-Jones virial result (upper abcissa, from Table II); for line shown ordinate is 1.01 times abcissa and correlation coefficient is 0.97.

Fig. 6. Correlation of parameters for Zeno and rectilinear diameter lines. Points from least-square fits given in Table I; lines described in text.

Fig. 7. Comparison of Zeno and rectilinear diameter lines for van der Waals equation, Lennard-Jones (6,12) potential, and hard core + square well potential. Points are from computer simulations cited in text; crosses pertain to two-dimensional case; solid lines computed from virial coefficients..

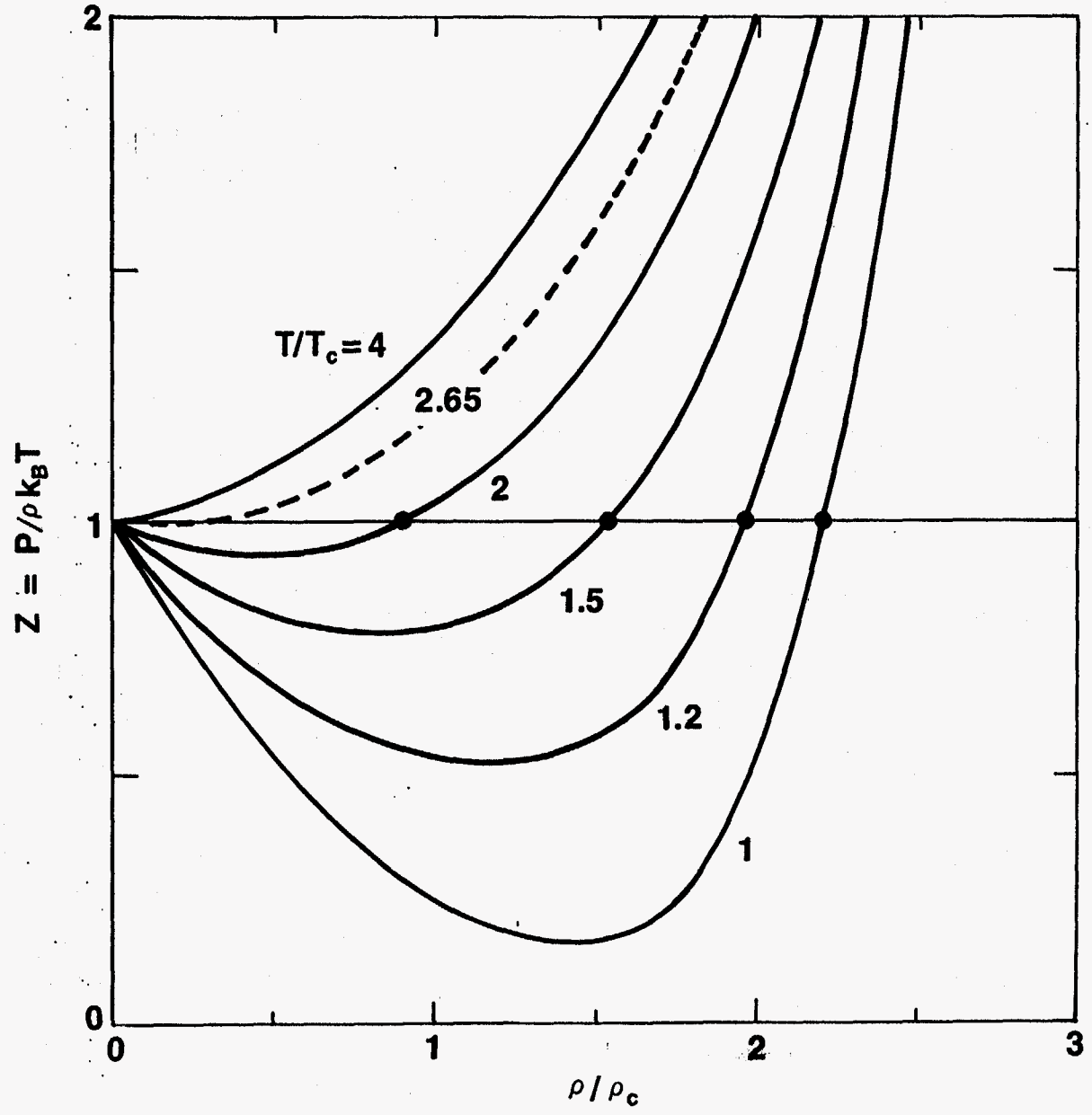
2
1
0
0
1
2
3
$Z = P/\rho k_B T$
ρ / ρ_c
$T/T_c = 4$
2.65
2
1.5
1.2
1

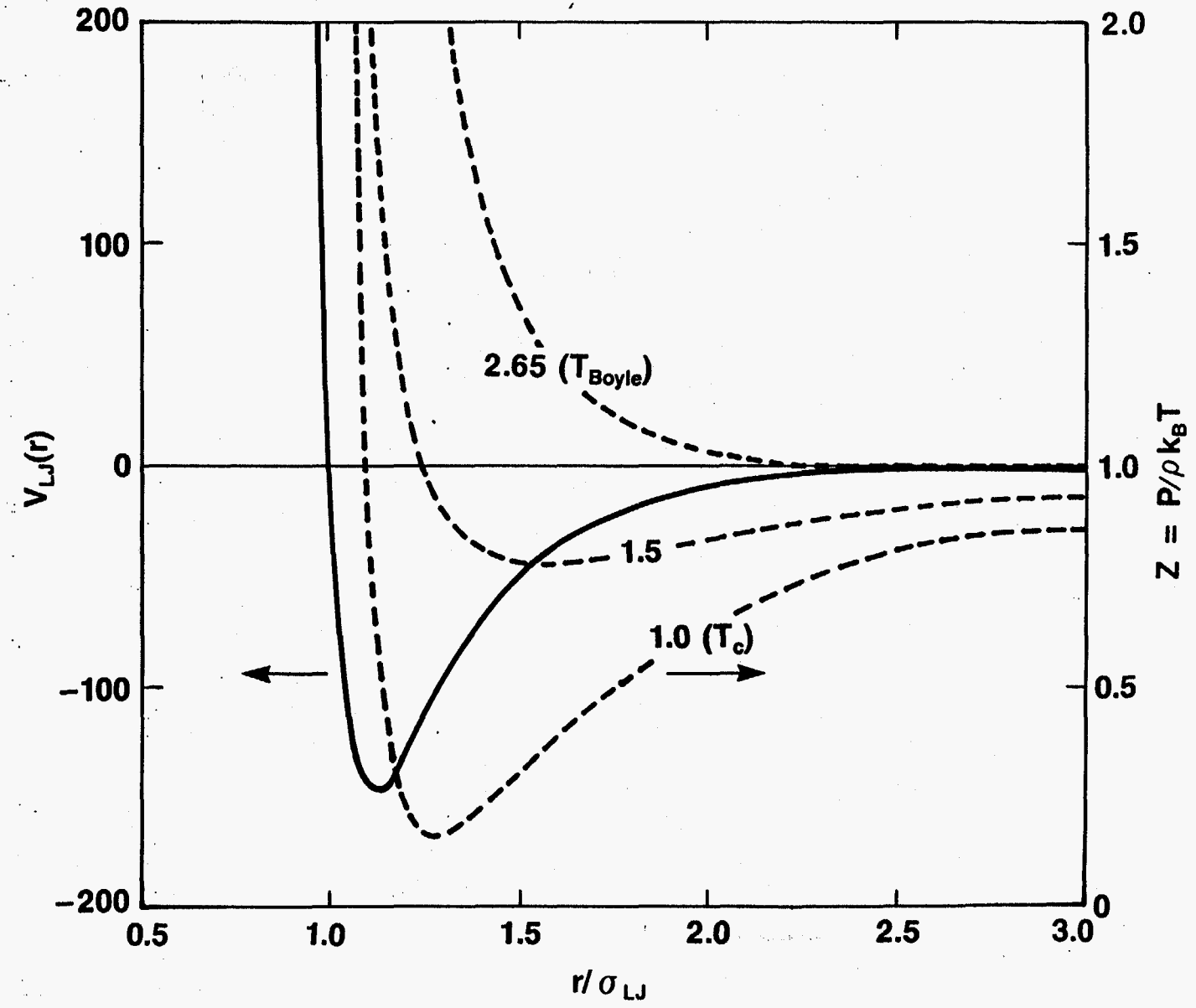
200
100
0
−100
−200
2.0
1.5
1.0
0.5
0
0.5
1.0
1.5
2.0
2.5
3.0
$V_{LJ}(r)$
$Z = P/\rho k_B T$
r/σ_{LJ}
2.65 (T_{Boyle})
1.5
1.0 (T_c)

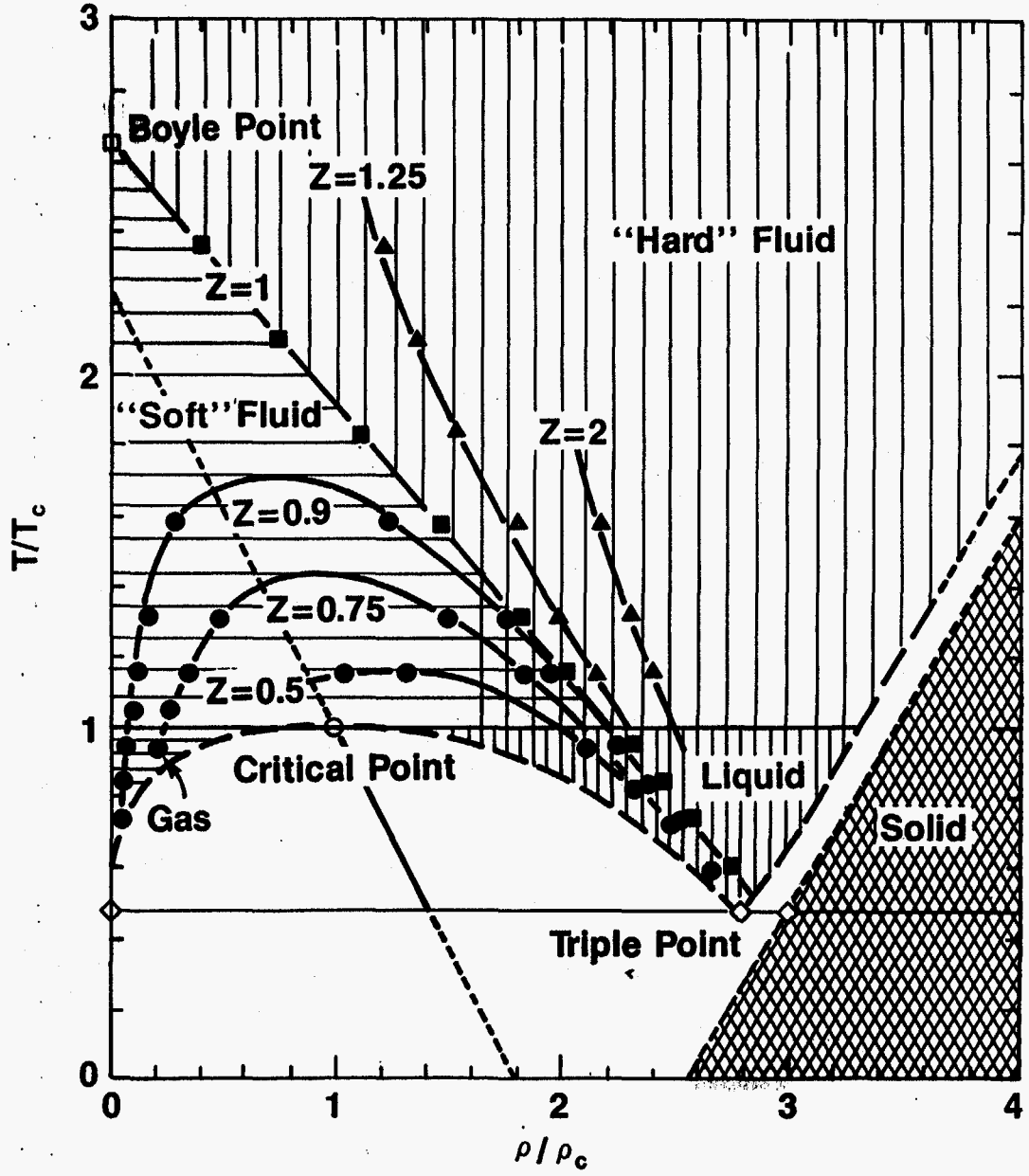
Boyle Point
Z=1.25
"Hard" Fluid
Z=1
"Soft" Fluid
Z=2
Z=0.9
Z=0.75
Z=0.5
Critical Point
Liquid
Gas
Solid
Triple Point
T/T_c
ρ/ρ_c
0
1
2
3
4

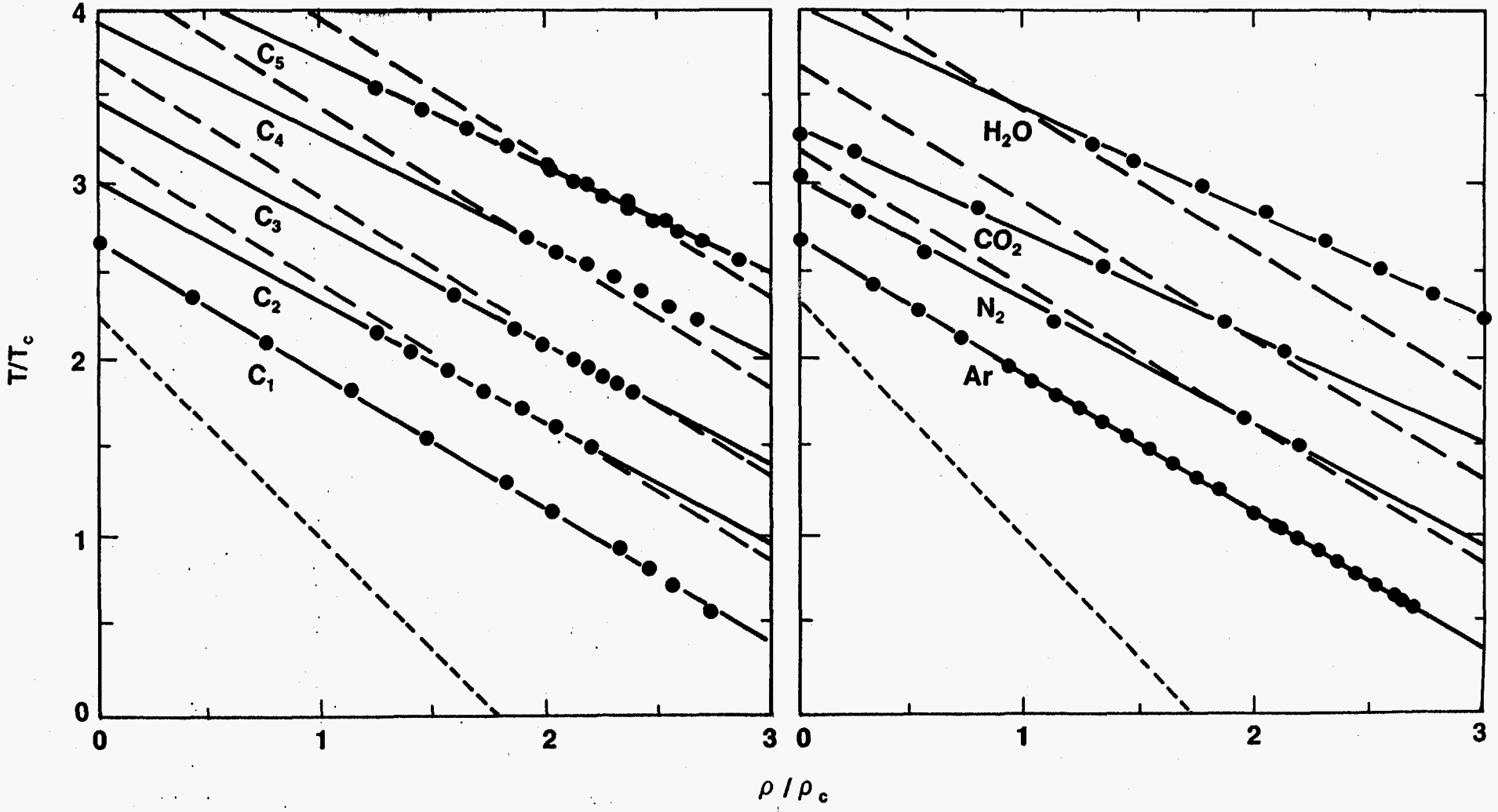
T/T_c
ρ / ρ_c
C5
C4
C3
C2
C1
H2O
CO2
N2
Ar
0
1
2
3
4

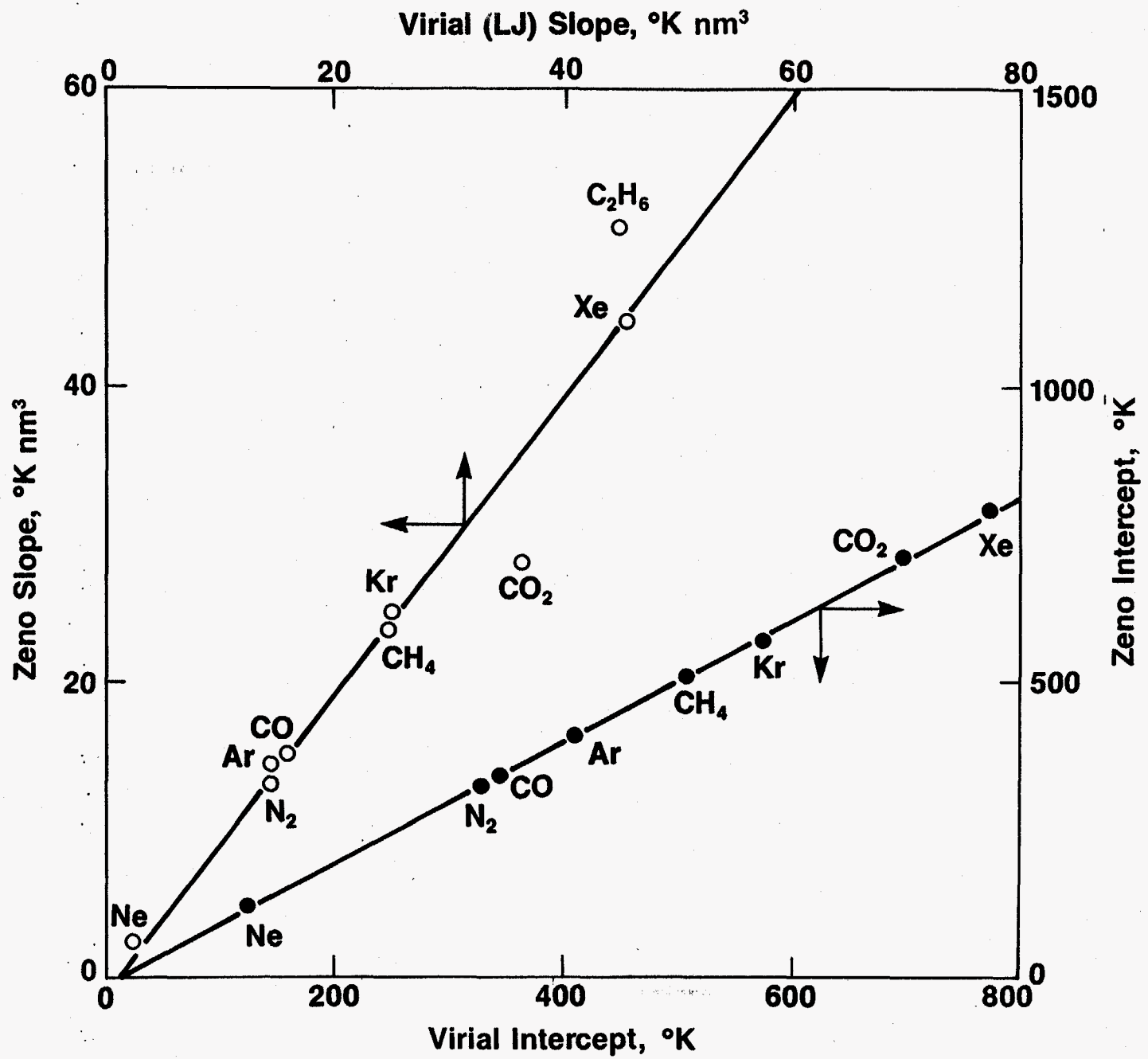
Virial (LJ) Slope, °K nm³
0
20
40
60
80
60
40
20
0
Zeno Slope, °K nm³
1500
1000
500
0
Zeno Intercept, °K
0
200
400
600
800
Virial Intercept, °K
C2H6
Xe
Kr
CO2
CH4
CO
Ar
N2
Ne
CO2
Xe
Kr
CH4
Ar
CO
N2
Ne

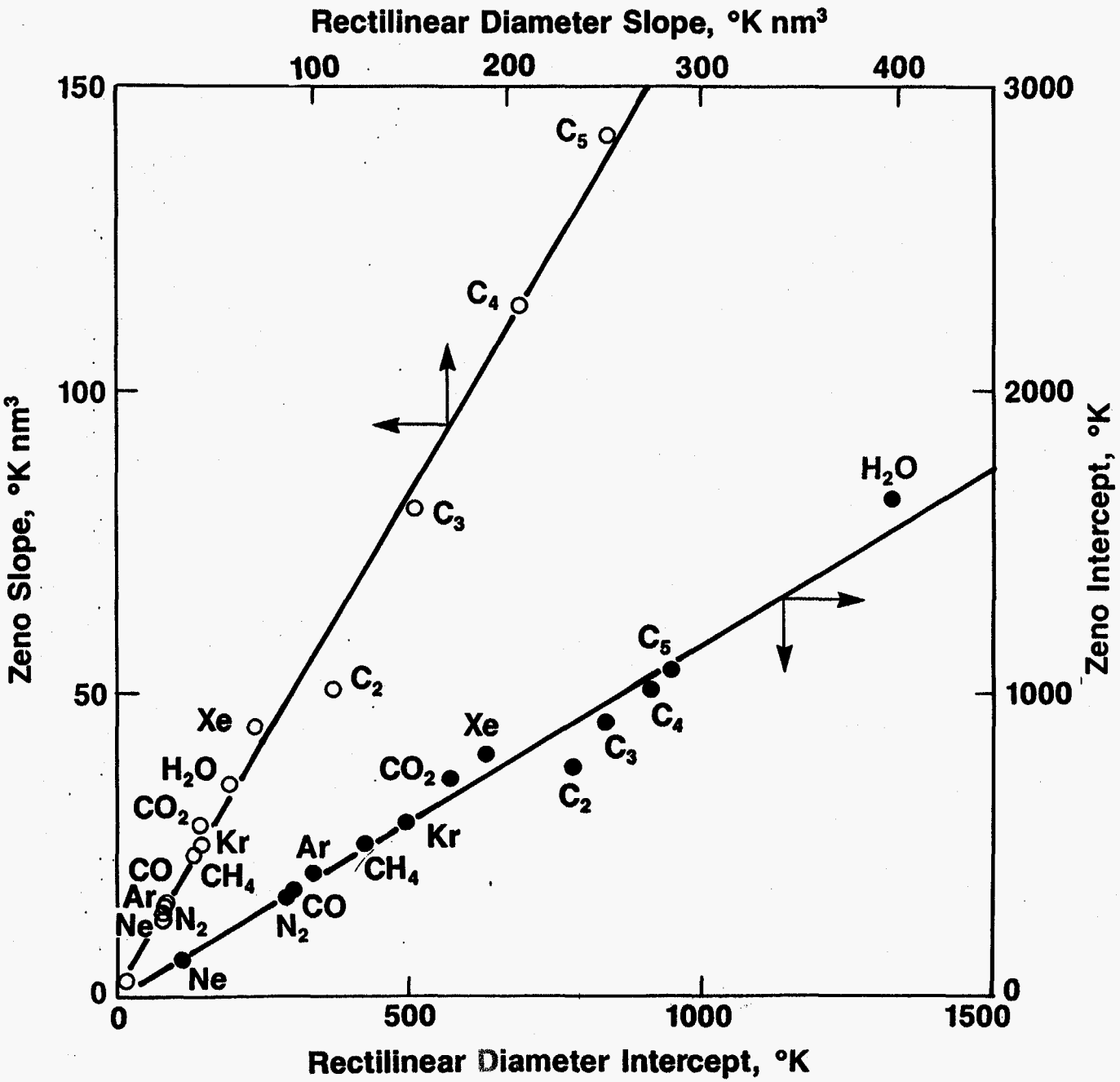
Rectilinear Diameter Slope, °K nm³
100
200
300
400
150
100
50
0
Zeno Slope, °K nm³
3000
2000
1000
0
Zeno Intercept, °K
0
500
1000
1500
Rectilinear Diameter Intercept, °K
C5
C4
C3
C2
Xe
H2O
CO2
Kr
CO
CH4
Ar
N2
Ne
C5
C4
C3
C2
Xe
H2O
CO2
Kr
Ar
CH4
CO
N2
Ne

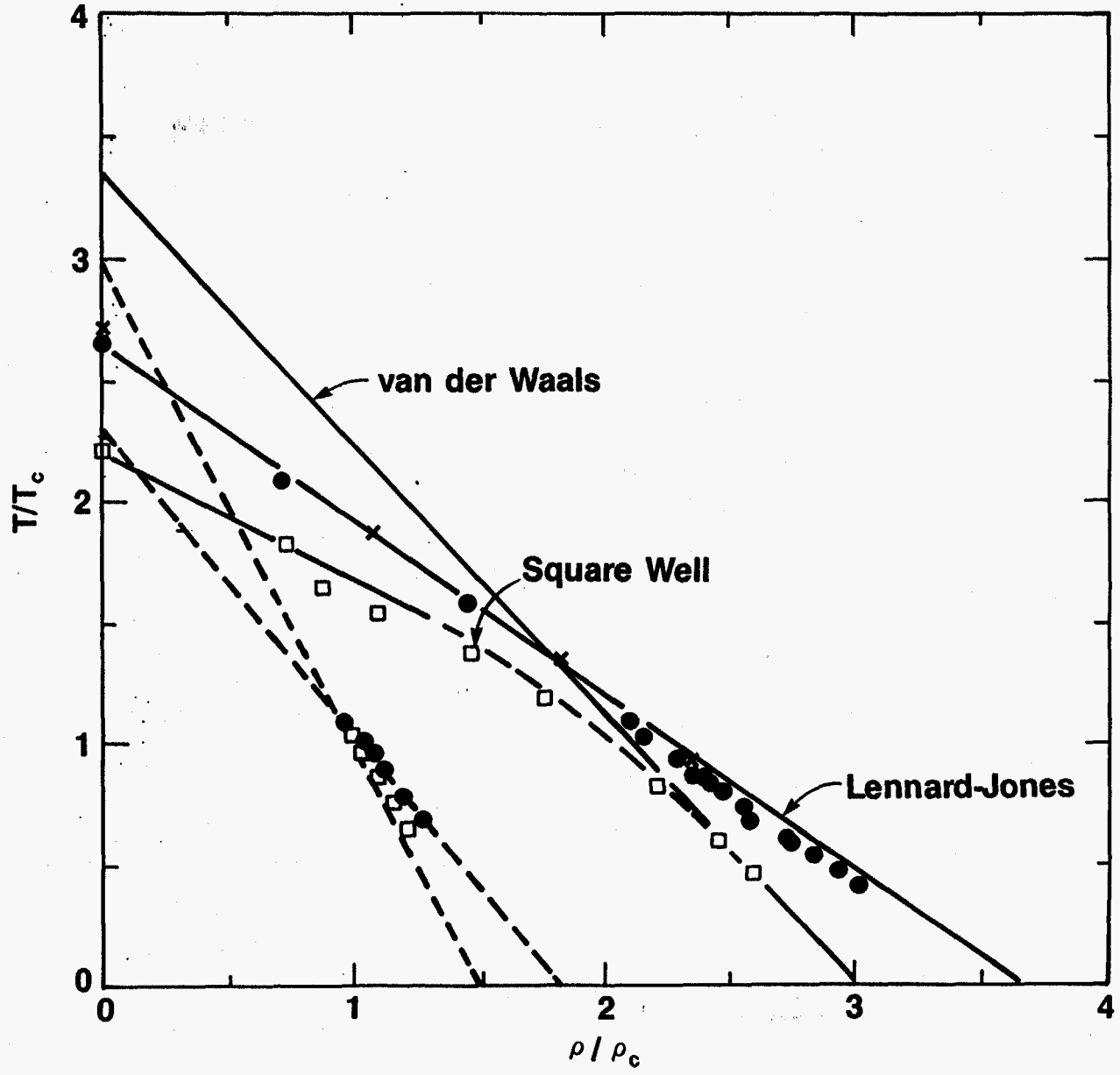
4
3
2
1
0
0
1
2
3
4
T/T_c
ρ / ρ_c
van der Waals
Square Well
Lennard-Jones

Table I. Critical Constants, Boyle Temperatures, Zeno and Rectilinear Diameter Lines[a]

Subs.	T_c	ρ_c	P_c	T_B	I_{RD}	$-S_{RD}$	I_Z	$-S_Z$
Ne	44.4	14.4	27.2	123 **2.77**	113 **2.53**	4.71 **1.53**	123 **2.77**	2.49 **0.810**
Ar	150.9	8.08	48.6	408 **2.70**	355 **2.35**	25.1 **1.35**	408 **2.70**	14.5 **0.777**
Kr	209.4	6.52	54.8	573 **2.74**	492 **2.35**	43.0 **1.34**	569 **2.72**	24.7 **0.769**
Xe	289.7	5.07	58.8	775 **2.68**	632 **2.18**	70.2 **1.23**	791 **2.73**	44.3 **0.775**
N_2	126.3	6.68	33.9	325 **2.57**	291 **2.31**	24.5 **1.30**	321 **2.54**	13.1 **0.693**
CO	132.9	6.47	35.0	342 **2.57**	298 **2.25**	25.3 **1.23**	341 **2.57**	15.2 **0.739**
CO_2	304.2	6.40	73.9	697 **2.29**	570 **1.87**	42.1 **0.89**	709 **2.33**	28.1 **0.591**
CH_4	190.6	6.05	46.2	506 **2.66**	425 **2.23**	38.9 **1.24**	505 **2.65**	23.5 **0.744**
C_2H_6	305.4	4.07	49.1	----	782 **2.56**	110 **1.59**	762 **2.50**	50.6 **0.674**
C_3H_8	370.0	3.09	42.7	----	834 **2.26**	152 **1.26**	902 **2.44**	80.7 **0.673**
C_4H_{10}	425.2	2.33	38.0	----	912 **2.15**	205 **1.13**	1017 **2.39**	114 **0.625**
C_5H_{12}	469.6	1.98	33.6	----	949 **2.02**	250 **1.03**	1073 **2.29**	142 **0.598**
H_2O	647.3	10.9	221.2	----	1327 **2.05**	57.5 **0.968**	1638 **2.53**	35.0 **0.588**
LJ[b]	**1.30**ϵ/k	**0.31**σ^{-3}		**2.60**	**2.30**	**1.30**	**2.60**	**0.728**

[a] Units are °K for temperature, 1000/Å^3 for density, bar for pressure. Quanties in boldface are dimensionless reduced parameters obtained by normalization to nominal T_c and ρ_c values. I denotes intercept, -S negative of slope. For H_2O both the Zeno and RD lines show appreciable curvature; parameters represent best linear fit.

[b] Parameters for Lennard-Jones (6,12) potential, derived from computer simulations cited in text.

Table II. Boyle Point and Zeno Slope from Lennard-Jones Parameters.[a]

Subs.	σ_{LJ}	ε_{LJ}	$T_B(LJ)$	$-S_Z(LJ)$
Ne	2.75	36	120 **2.70**	2.24 **0.728**
Ar	3.41	119	408 **2.70**	14.1 **0.775**
Kr	3.68	167	571 **2.73**	24.9 **0.776**
Xe	4.07	225	769 **2.65**	45.4 **0.794**
N_2	3.70	95	325 **2.57**	14.4 **0.762**
CO	3.76	100	342 **2.57**	15.9 **0.774**
CO_2	3.91	203	694 **2.28**	36.3 **0.764**
CH_4	3.82	148	506 **2.66**	24.7 **0.789**
C_2H_6	3.95	243	831 **2.72**	44.8 **0.646**
C_3H_8	5.64	242	828 **2.24**	130 **1.07**
C_4H_{10}	4.97	297	1016 **2.16**	109 **0.449**
LJ			**2.63**	**0.713**
SW			**2.21**	**0.520**

[a] Units and notation as in Table I, except for radius parameter σ, which is in Å. Values of σ and ε from Ref. 23, derived from second virial coefficient data. Boyle temperature T_B and Zeno slope S_Z computed from theoretical virial coefficients for LJ potential or (bottom line) square well potential.

Table III. Triple point parameters.[a]

Subs.	T_t	P_t	ρ_t(vap)	ρ_t(liq)	ρ_t(sol)	ρ_t(Z)	ρ_t(RD)
Ar	83.78	0.688	0.0619	21.32	23.82	22.36	21.61
	0.555		**0.0077**	**2.64**	**2.95**	**2.76**	**2.66**
N_2	63.15	0.125	0.0145	18.65	19.89	19.68	18.60
	0.500		**0.0022**	**2.79**	**2.97**	**2.94**	**2.78**
CH_4	90.68	0.117	0.0094	16.94	18.22	17.63	17.19
	0.476		**0.0015**	**2.78**	**2.99**	**2.92**	**2.83**
CO_2	216.58	5.185	0.192	16.12		17.49	16.79
	0.7120		**0.0300**	**2.52**		**2.74**	**2.60**

[a]Units and notation as in Tables I and II; data from Ref. 20.

Here ρ_t(Z) denotes density computed from Zeno line at T_t, ρ_t(RD) that from Eq.(6) of text.

Table IV. VdW Coexistence Curve and Rectilinear Diameter Line

T/T_c	ρ_V/ρ_c	ρ_L/ρ_c	Z_V	Z_L	$\bar{\rho}/\rho_c$	$\bar{\rho}/\rho_c$[a]
1	1	1	0.375	0.375	1	1
0.98	0.7267	1.289	0.485	0.274	1.008	1.010
0.95	0.5790	1.462	0.554	0.219	1.021	1.025
0.9	0.4257	1.657	0.633	0.163	1.041	1.050
0.8	0.2397	1.933	0.750	0.0933	1.086	1.100
0.7	0.1280	2.140	0.839	0.0491	1.134	1.150
0.5	0.0217	2.259	0.959	0.0125	1.239	1.250
0.3	0.0040	2.704	0.999	0.0025	1.352	1.350
0.2	0.0000	2.810	1.000	0.0008	1.405	1.400
0	0	3	1	0	1.5	1.5

[a]Nominal linear approximation, from Eq.(5) of text.